宇宙線中の一次電子と超新星加速

Nov.18/04 西村 純

- Some Historical Aspect
- Early Study
- Astrophysical Significance of primary Electrons
- Super Nova Accelerations
- Effect of Nearby Sources

Some Historical Aspect

~1930

- **Positron** — **Anderson (1932)**
- **E-W Asymmetry (Plus Charge)** — **Alvarez (1933)**
- **Increase of Cosmic-ray Flux around 15km** — **Pfotzer (1936)**
- **Cascdae Theory**

  Bhabha-Heitler (1937) & Carlson -Oppenheimer(1937)
- **Positrons as Primary Cosmc ray s** — **Euler-Heisenberg (1938)**

~1940

- **Protons as Primary Cosmic rays** — **Schein Jose Wollan (1941)**

Astrophysical Aspect

● Galactic Radio Wave	Jansky (1931)
● Super Novae Origin	Zwiky (1934)
	Ginzburg (1953)
	Hayakawa(1956)
● Electron Synchrotron	Alfven(1950)
	Ginzburg (1951)
● Polarization of Optical light from Crab	Shchlovsky(1953)

Interactions During the Propagation inside the Galaxy

- Inverse Compton **Feenberg & Primakov (1949)**

- Secondary Electrons **Hoyle, Hayakawa(1952)・・・・・・**

CR + Intersteller matter

⇨ $\pi^{\pm} \Rightarrow \mu^{\pm} + \nu = e^{\pm} + \nu + \nu$

Problems related Primary Electrons

1960 ●Direct Observations e/P ~1%

●Primary or Secondary Origin e +/e- ~10%

~1965 ●Observations Electrons beyond 100GeV

●Bending of the spectrum

1980 以降

●Electrons beyond 1TeV

●Relation to the Nearby sources

Difficulties of the Observations of Primary Electrons

- **Low Flux** => **Large SΩ**

  Flux ~1/ 100m2sr.sec E>100GeV

  ~2/m2.sr.day E>1TeV

- **Identification of Electrons** => **Rejection Power to proton 10^{-4} ~10^{-5}**

  10-100GeV e/P <1%

  1TeV e/P <0.1%

- **Precise Energy Determination** => **Massive Detectors**

Instruments for Electron Observations

Earl (1960)

VOLUME 6, NUMBER 3 PHYSICAL REVIEW LETTERS FEBRUARY 1, 1961

Table I. Data on the balloon flight and the cloud chamber.

Balloon flight	
Date:	May 12, 1960
Location:	Minneapolis, Minnesota (geomagnetic latitude 55°N)
Time at ceiling:	12 hours
Pressure altitude:	4 to 6.5 g cm^{-2}. Average: 4.5 g cm^{-2}
Multiplate cloud chamber	
Number of lead plates:	5
Thickness of plates:	0.6 cm - 7.5 g cm^{-2} (1.1 radiation lengths)
Sensitive time per picture:	(0.19 ±0.01) sec
Geometric factor for region bounded by illuminated areas of top and bottom:	(33.5 ±1.5) cm^2 sr

Shower events in which there was no trace of a track in the top section even though the axis was well illuminated were assumed to be initiated by gamma rays. There is no reason to believe that the upper section was insensitive at any time during the flight. The procedure used to determine

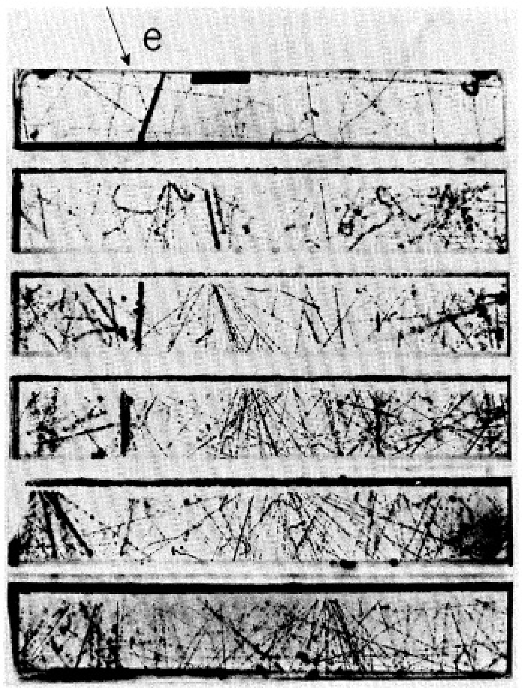

FIG. 1. A cloud-chamber picture of a shower produced by a high-energy electron. The incident electron is visible in the top section of the cloud chamber.

Muller & Meyer (1973)

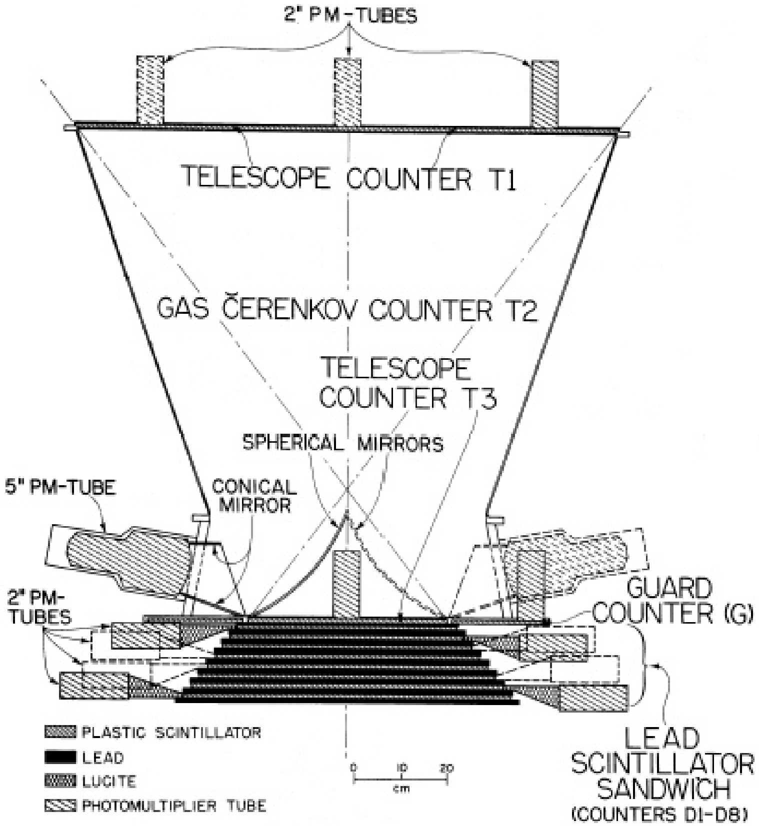

FIG. 2.—Schematic cross-section of the detector

Prince (1976)

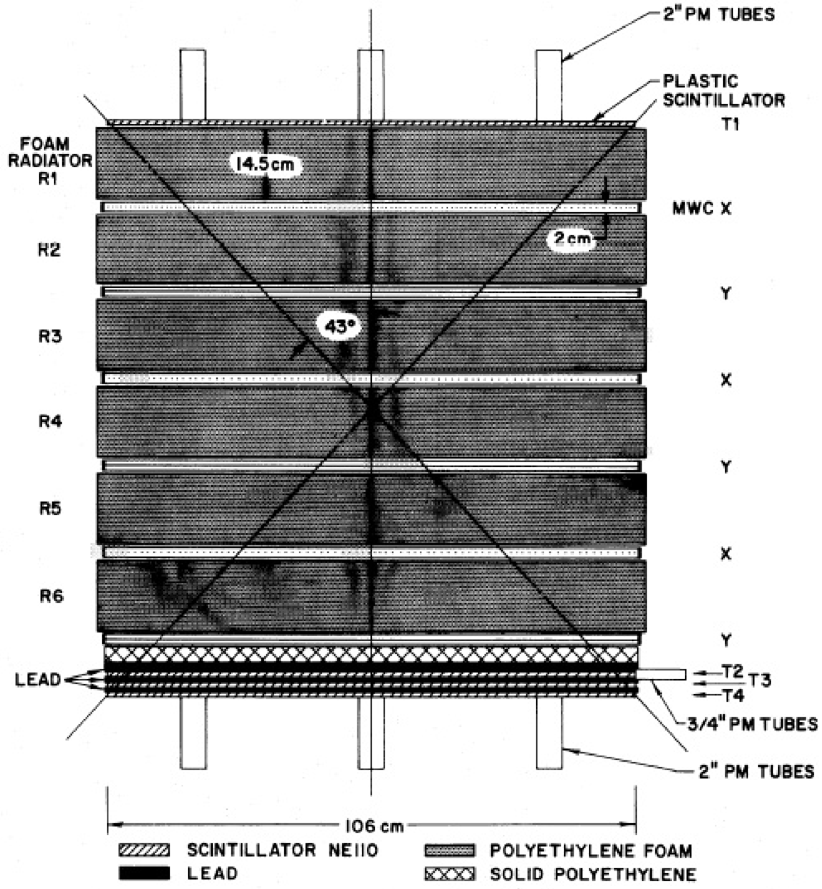

FIG. 1.—Schematic cross section of the instrument

ECC (1968-)

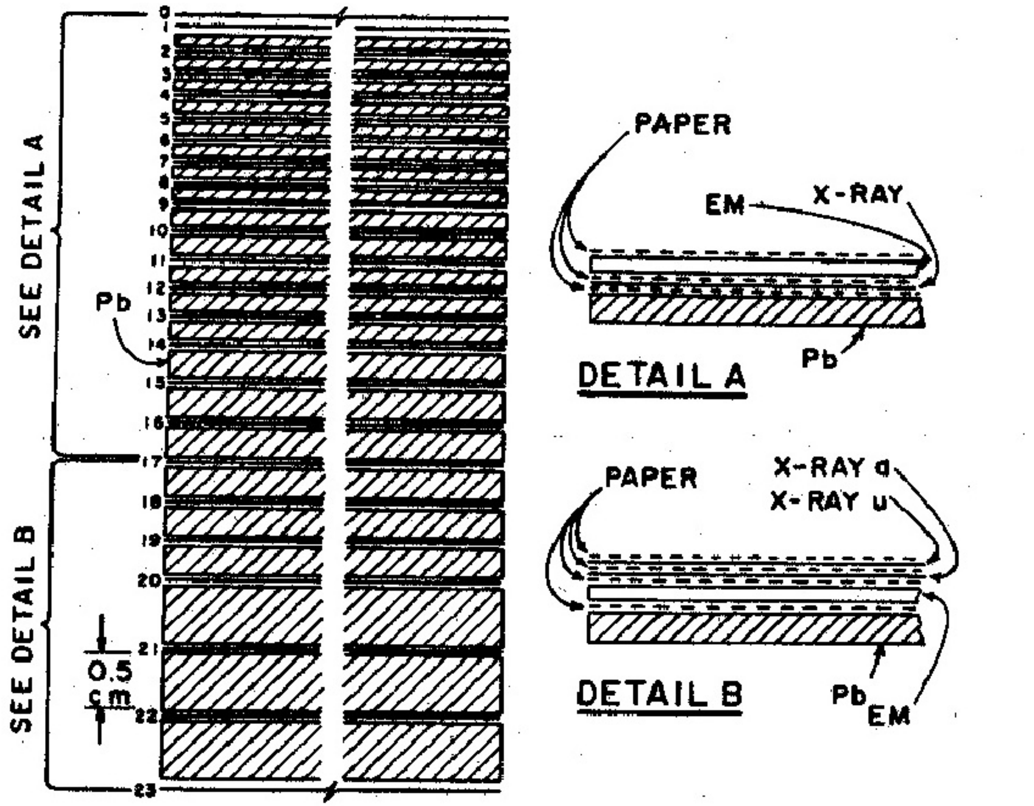

FIG. 1.—Emulsion chamber configuration for 1968 flight (*top*) and 1976 flight (*bottom*)

1980 年代の電子スペクトル

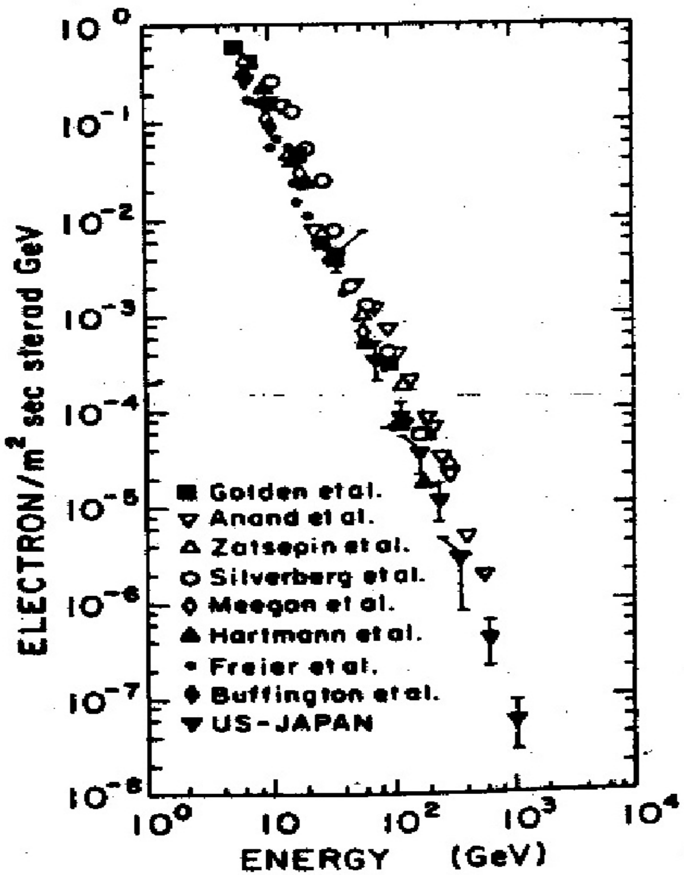

FIG. 4.—Differential energy spectrum of primary electrons (conventional plot).

最近の観測器

● ECC (MSC)	Emulsion
● BETS	Imaging Calorimeter
● HEAT	Magnet Spectrometer
● Caplice	Magnet Spectrometer
● AMS 0-1 (Shuttle)	Magnet Spectrometer
● ATIC	Deep Calorimeter
● Calet (ISS)	Deep Calorimeter
● AMS (ISS)	Magnet Spectrometer

Electron & Gamma-Ray Observation with BETS

BETS: Balloon borne Electron Telescope with Scintillating fibers

- Development of SciFi/lead imaging calorimeter for electrons
  NIM 457, 499-508 (2001)
- Successful observation of electrons in 10-100 GeV
  ApJ 559, 973-984 (2001)
- Observation of atmospheric gamma-ray flux with improved BETS
  Phys Rev D 66, 052004(1-9) (2002)

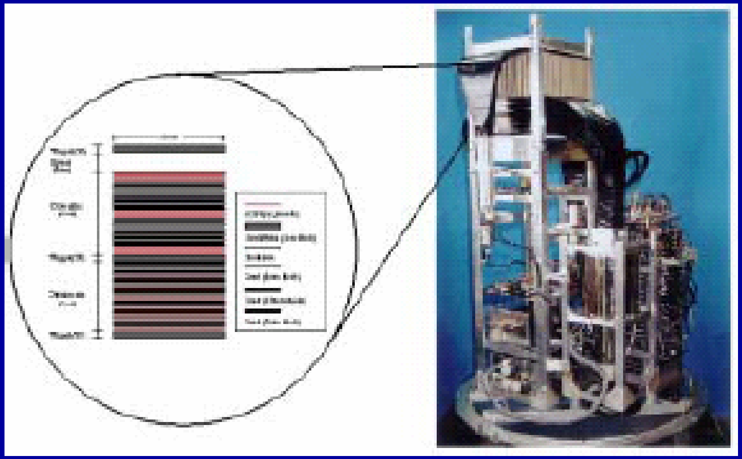

BET Instrument

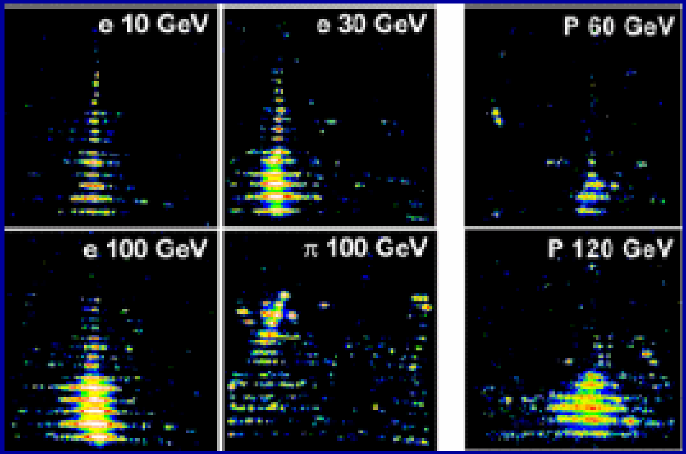

Shower Image at CERN

PPB-BETS：

Torii,S.: PSB1-0046

Automatic Tracing Tracks in each layer of ECC

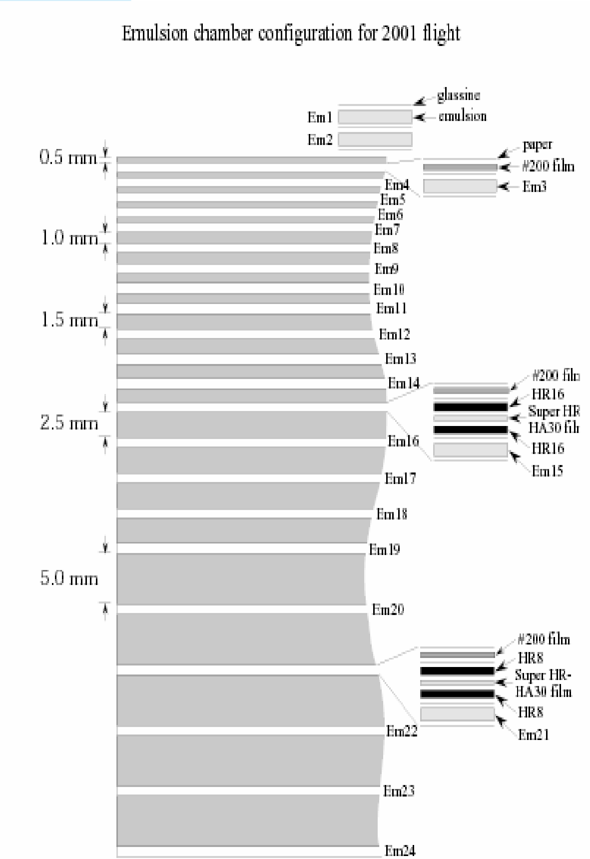

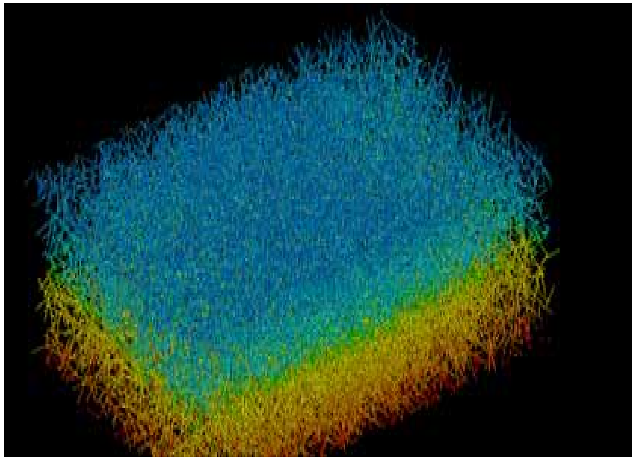

2cmx3cmx5Xo depth

~40hr Exposure at Balloon Altitude

Detected showers in MSC energy beyond 10GeV

Aoki.S et al : PSB1-0051

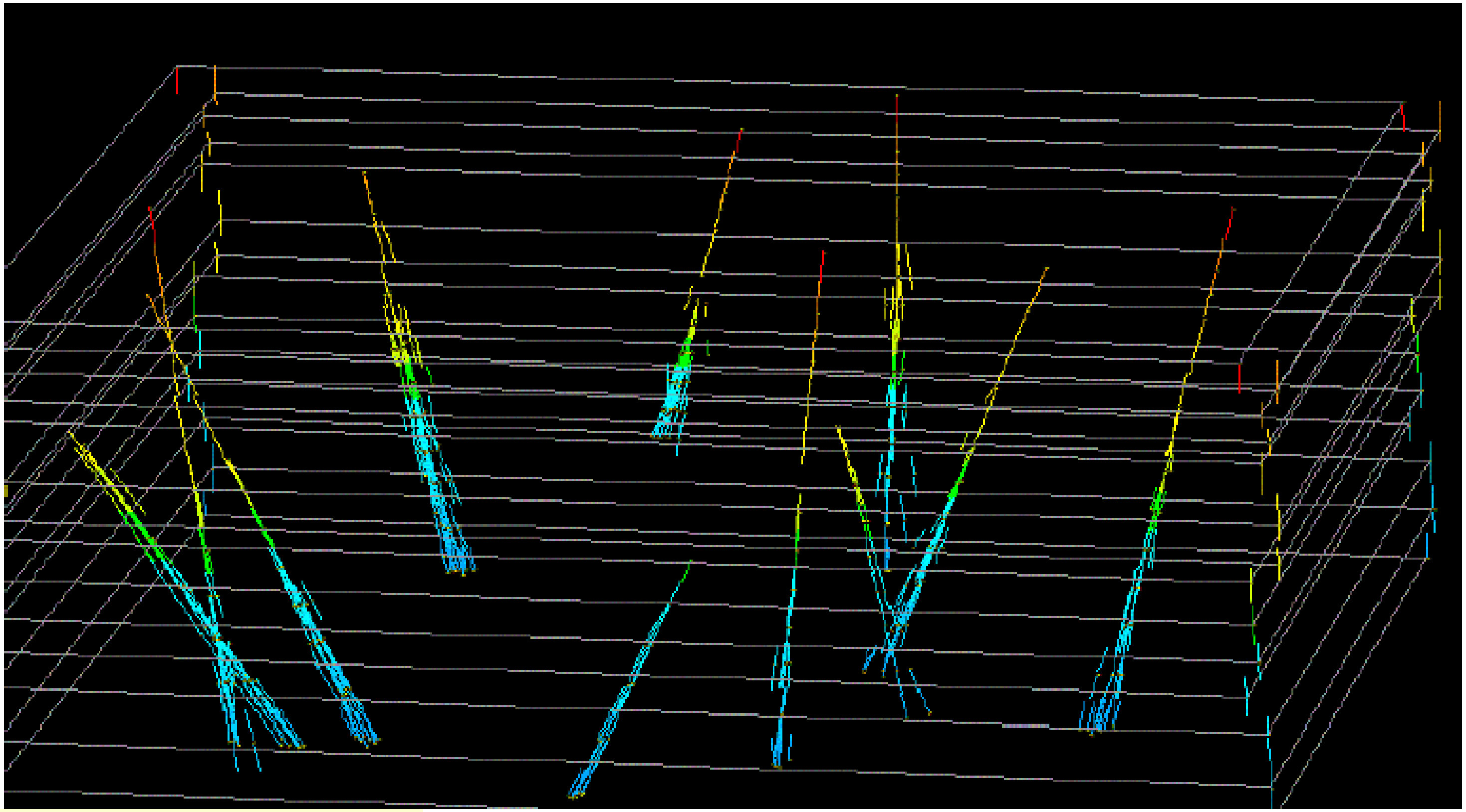

● Recently Observed Electron Spectrum

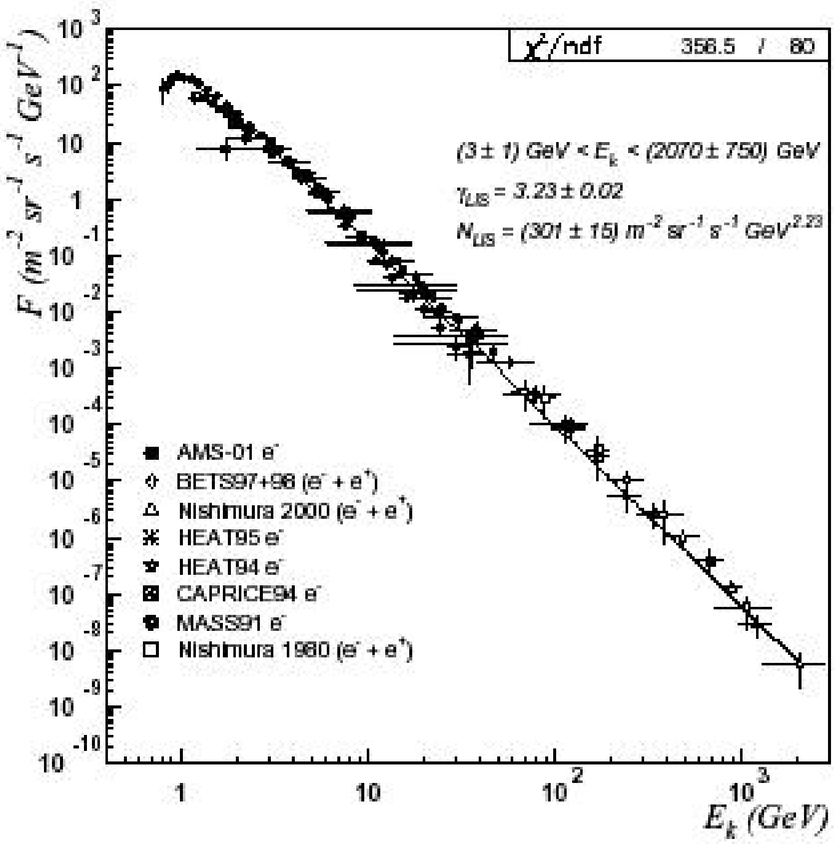

Fig. 9.— Local interstellar flux of electrons measured by the most recent experiments plus high energy data from Nishimura et al. (1980) (see table 1).

D.Casadei and V. Bindi: Astro-ph/ 0302307

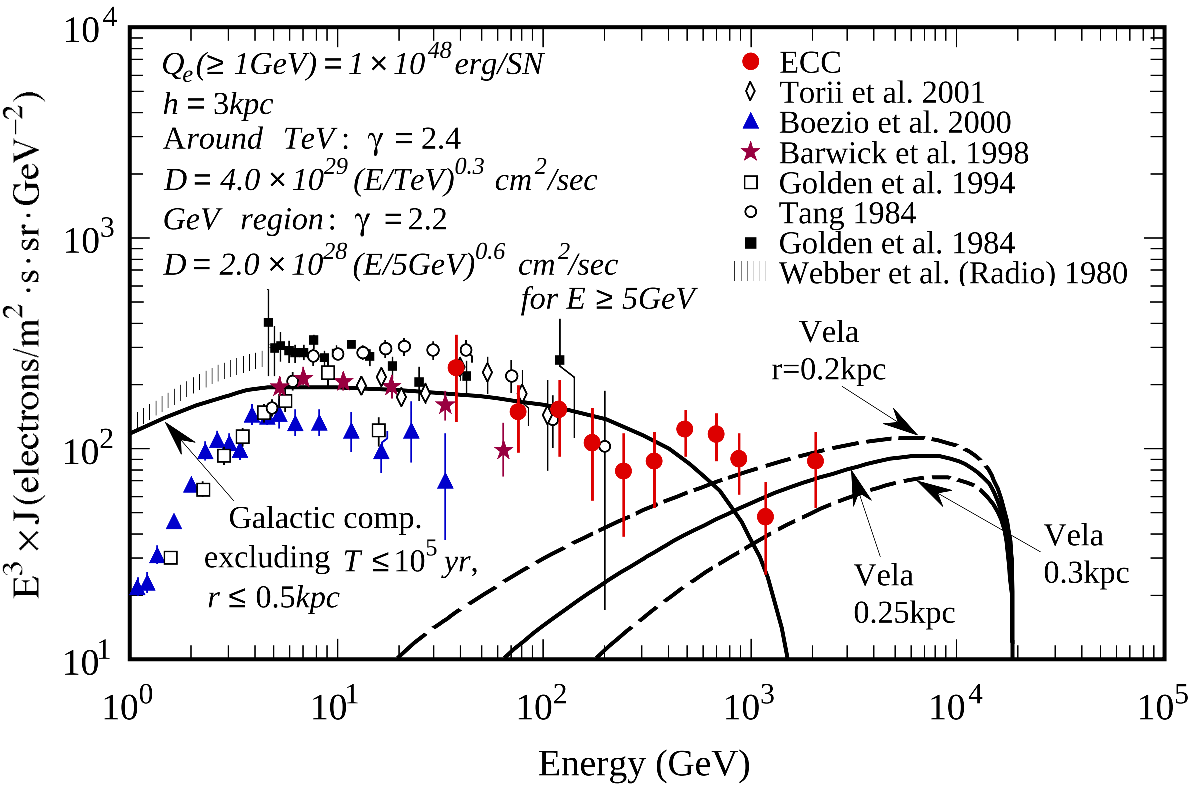

$Q_e(\geq 1GeV) = 1 \times 10^{48} erg/SN$
$h = 3kpc$
Around TeV: $\gamma = 2.4$
$D = 4.0 \times 10^{29} (E/TeV)^{0.3}\ cm^2/sec$
GeV region: $\gamma = 2.2$
$D = 2.0 \times 10^{28} (E/5GeV)^{0.6}\ cm^2/sec$
for $E \geq 5GeV$
ECC
Torii et al. 2001
Boezio et al. 2000
Barwick et al. 1998
Golden et al. 1994
Tang 1984
Golden et al. 1984
Webber et al. (Radio) 1980
Vela
r=0.2kpc
Vela
0.25kpc
Vela
0.3kpc
Galactic comp.
excluding $T \leq 10^5\ yr$,
$r \leq 0.5kpc$
$E^3 \times J$ (electrons/m$^2 \cdot$s$\cdot$sr$\cdot$GeV^{-2})
Energy (GeV)

● 宇宙線超新星起源説

1. エネルギーからの考察 (Ginzburg ,1953)

Volume of Galaxy:$V=10^{67}$cc CR Energy Density : $\rho \sim 1$eV/cc Total Energy = $\rho V \sim 10^{55}$erg

Rate of Loss = $\rho V/T = 10^{48}$erg/yr

for SN rate of 100yr, Each SN Out put =$(\rho V/T)(\text{SNrate}) \sim 10^{50}$erg

2. スペクトルの形 (Axford 1977)

● Shock Acceleration; r =Compression ratio

$E^{-(r+2)/(r-1)}dE \sim E^{-2}dE$ fro Strong Shock r=4

3. Evidence

- Radio and Optical wave from SNR,
- SN1006: X, & Gamma rays

●エネルギー損失

- **Synchrotron Process; Energy loss / sec**

$$\frac{4}{3}\sigma_T\left(\frac{E}{mc^2}\right)^2\left\langle\frac{H^2}{8\pi}\right\rangle C$$

H~5 μ Gauss

- **Inverse Compton: Energy loss / sec**

$$\frac{4}{3}\sigma_T\left(\frac{E}{mc^2}\right)^2\rho C$$

ρ ： energy density of Photons(3k, IR optical ・・・) ~1eV/cc

- **Life**: $\varepsilon = \rho + H^2/8\pi \sim 1$ eV/cc

T=3x10^{8}yr /(ε E) (eV/cc.GeV)

- **Propagation**

Diffusion Model

$$\frac{\partial f}{\partial t} - \quad (D \quad) f - \frac{\partial b E^2}{\partial E} = Q(r,z)$$

D: Do(E/Eo)$^{\delta}$

b: Energy loss Parameter

Q: Qo exp(-z/zo),

ho: Halo Thickness

zo: Disc thickness

- Travel Distance by Diffusion

R~(2DT)$^{1/2}$

Diffusion Constant

D=$D_o(E/E_o)^{\delta}$

- **E=1-100GeV**

Do~2×10^{28}cm^2/sec (B/C, HEAO— C ・・・)

$\delta \sim$ **0** **E<5GeV**

$\delta \sim$ **0.6** **E>5GeV**

- **E>100GeV (Anisotropy, B/C Runjob)**

$\delta \sim$ **0.3** **E~1TeV**

$$D=(1\text{-}5)\times10^{29}(E/\mathrm{TeV})^{0.3}\ \mathrm{cm^2/sec}$$

$$T=3\times10^{8}\mathrm{yr}/(\varepsilon E)\ (\mathrm{eV/cc.GeV})$$

● TeV 領域の電子

E>1TeV,

Life **T<3x105yrs**

Travel Distance **$R<(2DT)^{1/2}$ ~ 0.5-0.7kpc**

高エネルギー電子には最近の Nearby Source しか寄与しない

Nearby SNRs

List of nearby SNRs.

SNR	R(kpc)	Age(yr)
SN185	0.95	1.8×10^3
S147	0.80	4.6×10^3
HB 21	0.80	1.9×10^4
G65.3+5.7	0.80	2.0×10^4
Cygnus Loop	0.44	2.0×10^4
Vela	0.30	1.1×10^4
Monogem	0.30	8.6×10^4
Loop1	0.17	2.0×10^5
Geminga	0.4	3.4×10^5

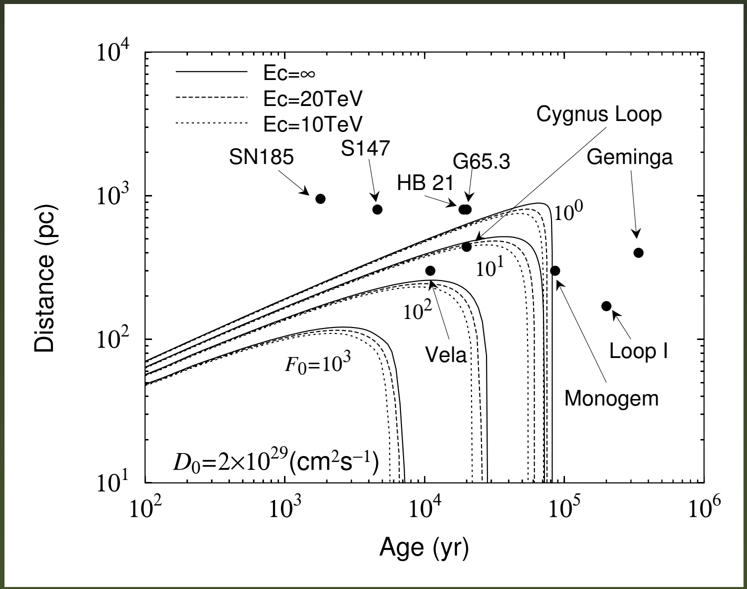

Contours of the electron flux $E^3 J$ at 3TeV between T and R

Source Spectrum $E^{-\gamma}$ Exp[-E/Emax]

B⊥ =5Gauss: T=1/(bE)=2.308x10^5 (TeV/E)yr

●Do=10^{29}(E/TeV)$^{\delta}$ cm^2/s

E=1TeV, Emax =10TeV, 20TeV

T=1/(bE)=2.308x10^5

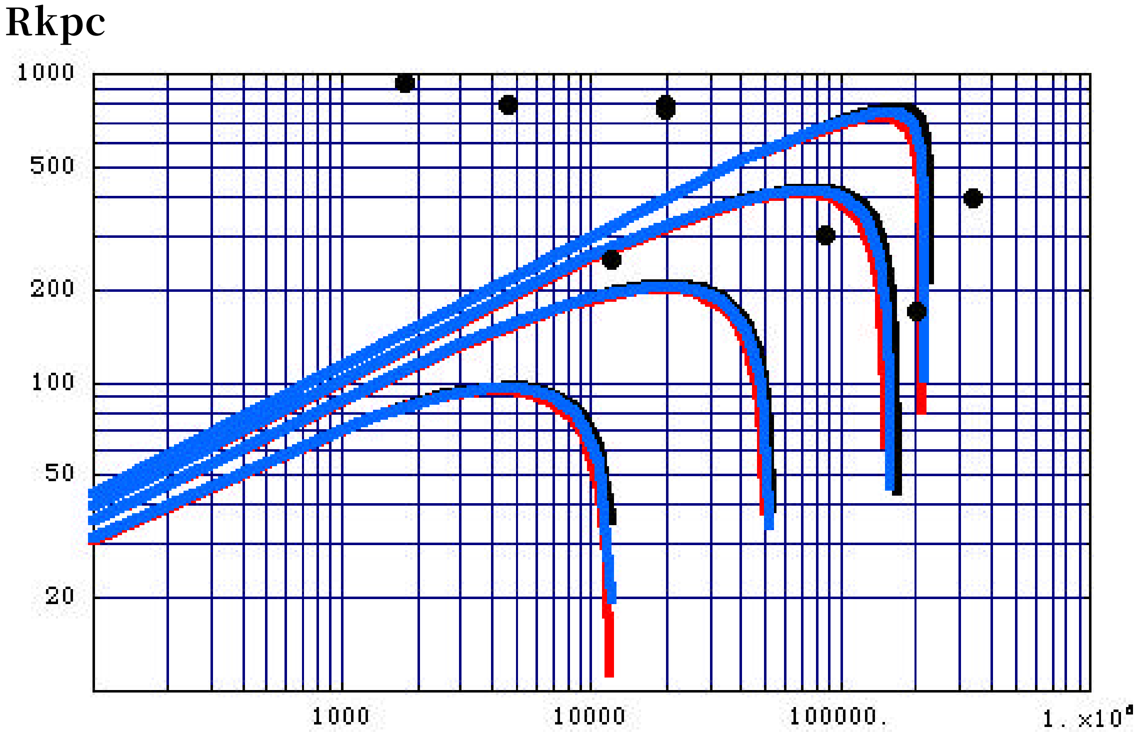

●E=1TeV, Contour Lines are 1.0,10,10^2,10^3 from the top

E2=10TeV

E2=20TeV

E2=∞:No cut

高エネルギー電子スペクトル

3/10/04　西村 純

T.Kobayashi et al. ApJ. ６０１, pp３４０－３５１, ２００４

- Observations => Low Flux => Large SΩT　　>100GeV 〜 1TeV

- Effect of Near by Sources　(Synchrotron, Inverse Compton,)

  ★Propagation => Limit by Distance and Life

  ★Acceleration: Electron Acceleration and Leakage

  ★Anisotropy :　ΔI/I 〜 Ri/Ti 〜 a few 10%

- Dark matter:　Dark matter Annihilation

  ★line spectrum => dE/E2 => hump

源から発生するスペクトル

●源の中：　　$E^{-\gamma}$ Exp[-E/Eo]　　○

●源からリークアウト

★時間的推移　　？
★スペクトルの形　　？

●その後の伝播　　△

●発生モデル　　？

★爆発時　Single Shot
★連続リーク
★最終崩壊　　(～10^5yr)

一次電子の遍歴

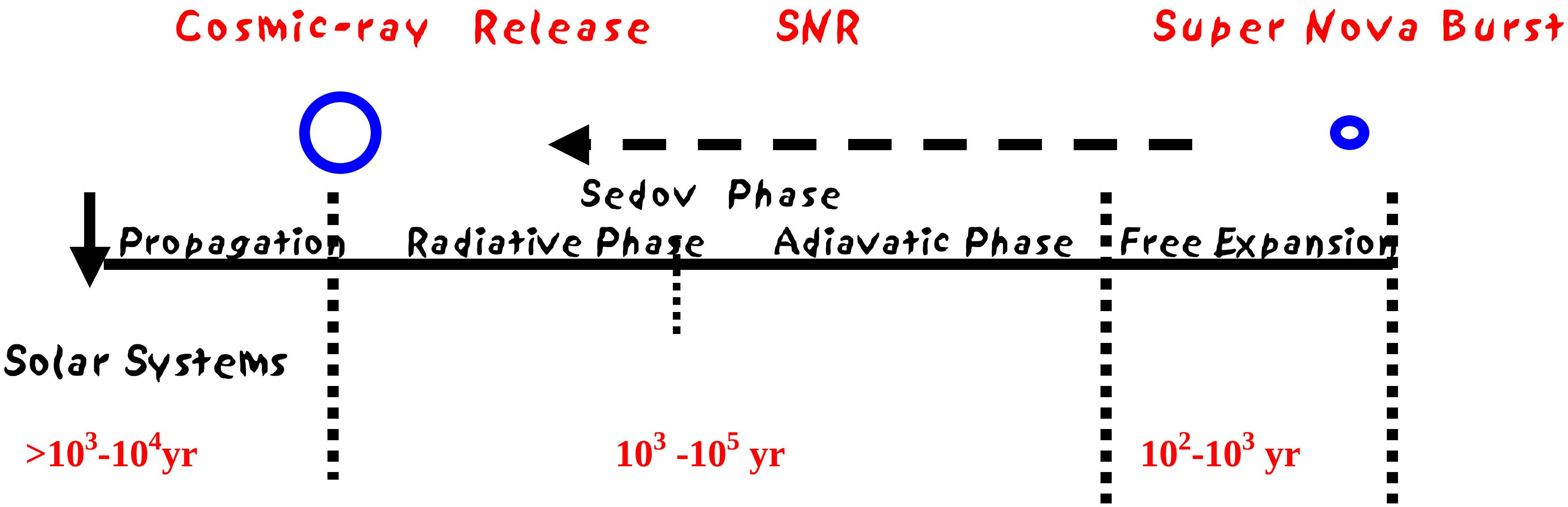

(R≧100pc)

$R=(2DT)^{1/2}$. $D\sim10^{29}cm^2/s$
$T\sim \mathbf{R}^2/((2D)$

No. of Nearby Source <100pc $=(100pc/15kpc)^2$ (!05yr/30yr)=0.15

2. Assumptions for Calculations

1, Total Output $Q_0(E>1\,\mathrm{GeV}) = 10^{48}$ erg/SN

2. DiffusionCoefficients $D = (1, 2, 4)\times 10^{29}(E/\mathrm{TeV})^{0.3}\,\mathrm{cm^2/s}$

3. $b = 1/2.3\times 10^{5}$ yr.TeV ($B \sim 5\,\mu$ Gauss)

4. Source Spectrum

$E^{-\gamma}\mathrm{Exp}[-E/E_c]$ (E_c = 10-100TeV)

5 Delay of Release after explosion τ , also continuous release

$\tau = 0,\ 5\times 10^{3}, 10^{4},\ 2\times 10^{4}, 5\times 10^{4}, 10^{5}$ yr

1. Nearby Sources used for Calculations

SNR	R(kpc)	$\pm\Delta$ R	To	Emax (TeV)
Vela	0.3kpc	$\pm$0.05	$1.1\text{x}10^4$yr	21TeV
Cygnus Loop	0.44	$\pm$0.05	$2.0\text{x}10^4$yr	2.6
Monogem	0.3	$\pm$0.05	$8.6\text{x}10^4$yr	2.6
Loop1	0.17	$\pm$0.05	$1.7\text{x}10^5$yr	1.15

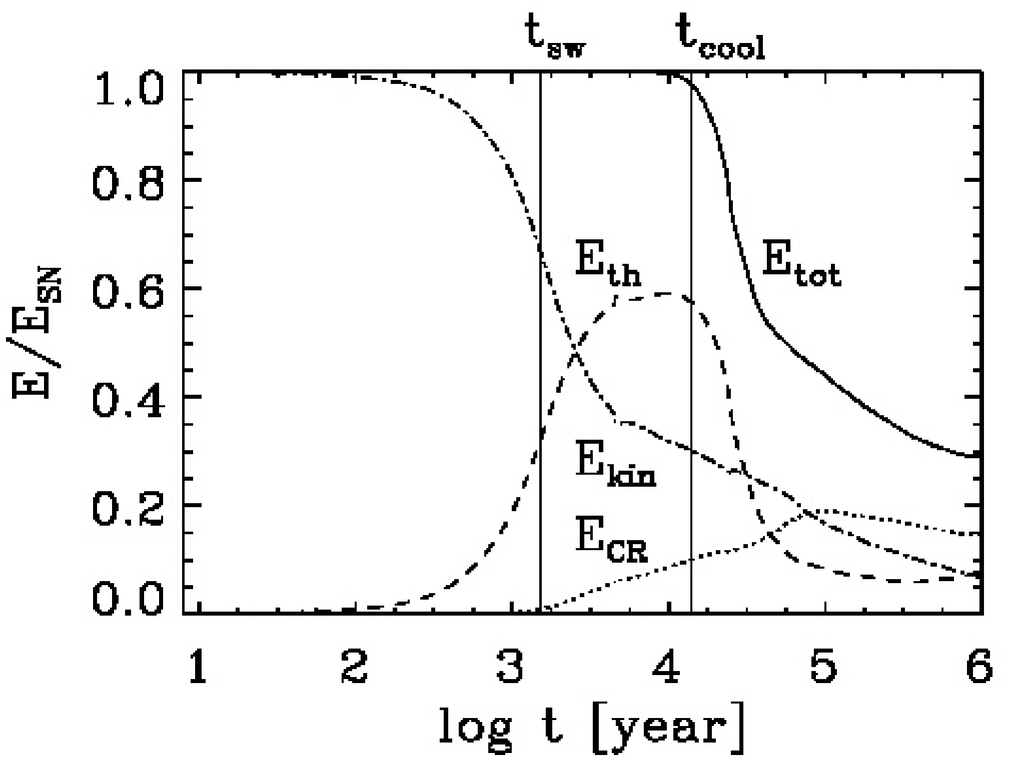

Figure 1. The different energy contributions in units of the initial SN-explosion energy E_{SN} for an external density of $n_{ext} = 1\,\mathrm{km\,s}^{-1}$ as a function of time. The two vertical lines denote the sweep-up time t_{sw} (Equation 4) and the time t_{cool} (Equation 5) when cooling becomes important and a dense shell is formed. For $t > t_{cool}$ the thermal energy E_{th} can be radiated away very effectively. During this cooling phase heating by Alfvén waves can still increase the total thermal energy associated by a decrease of the total cosmic ray energy E_{CR}

Dorfi 2000 ASS.272:p227

Using the model described in § 2, we investigated the evolution of the nonthermal photon spectra from SNRs by assuming a variety of initial conditions. Specifically, we modeled Type I ($M_{ej} = 1.4\ M_{\odot}$, $v_0 = 10^9$ cm s^{-1}) supernovae expanding into an ISM with a density of 0.1, 1, or 10 hydrogen atoms cm^{-3} and Type II ($M_{ej} = 10\ M_{\odot}$, $v_0 = 3.7 \times 10^8$ cm s^{-1}) supernovae expanding into an ISM with a density of 1 hydrogen atom cm^{-3}. Thus, the initial bulk kinetic energy is the same for the Type I and Type II SN models. We adopt a particle source normalization such that 10% of the initial bulk kinetic energy of the supernova ejecta is transferred to both cosmic-ray electrons and protons prior to the SNR entering the radiative phase, after which we assume that particle acceleration ceases. The evolution of the particle and photon spectra for each model is shown in Figures 2, 3, 4, 5, 6, 7, 8, and 9 (see the figure captions for details).

The general characteristics of the photon spectra shown in Figures 3, 5, 7, and 9 are as follows:

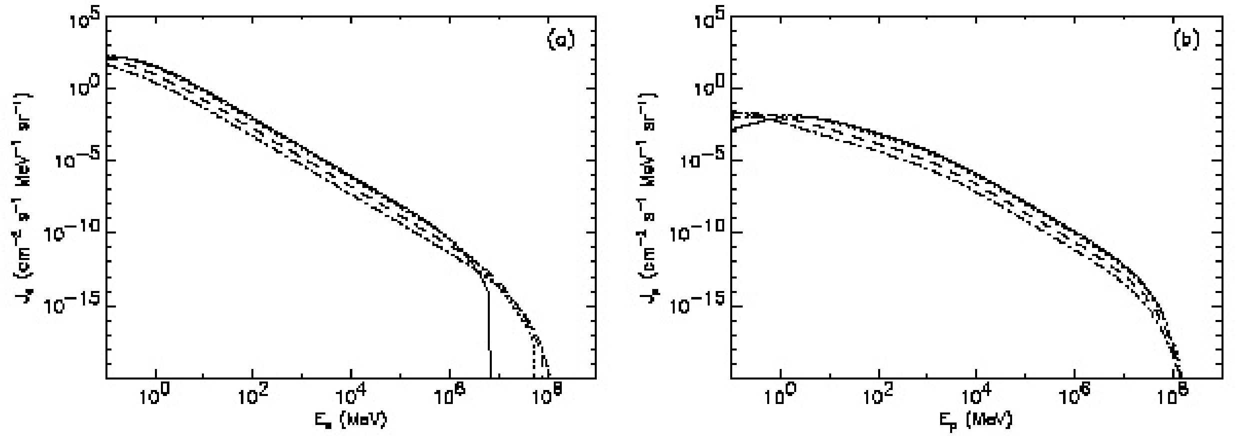

FIG. 2.—The isotropic particle intensities (*a*) J_e and (*b*) J_p at 500 (*dot-dashed curves*), 5000 (*dashed curves*), 50,000 (*dotted curves*), and 100,000 yr (*solid curves*) for $n_{ISM} = 0.1$ cm^{-3}, $M_{ej} = 1.4\ M_{\odot}$, $v_0 = 10^9$ cm s^{-1}, $B_{ISM} = 5\ \mu$G, and a source spectral index $\alpha = 2$. For these parameters, the particle sources turn off at $t = t_{rad} = 9.6 \times 10^4$ yr. The sharp cutoff in the electron intensity at high energies and late times is due to synchrotron losses, while the turnover at low energies in both the electron and proton intensities is due to Coulomb losses.

Sturner eta al ApJ. 1997. 490.p619 e & P in SNR with Evolution time

TABLE 2

ROLLOFF FREQUENCY AND MAXIMUM ELECTRON ENERGY UPPER LIMITS

Object	$\nu_{rolloff}$ (10[16] Hz)	$\nu_{rolloff}$ (keV)	$E_{max}[(B/10\mu G)]^{1/2}$ (ergs)	$E_{max}[(B/10\mu G)]^{1/2}$ (TeV)
Kes 73[a]	150	6	290	200
Cas A.............	32	1	130	80
Kepler	11	0.5	79	50
Tycho	8.8	0.4	70	40
G352.7−0.1......	6.6	0.3	60	40
SN 1006[b].........	6	0.2	57	40
3C 397............	3.4	0.1	43	30
W49 B............	2.4	0.1	36	20
G349.7+0.2......	1.8	0.07	31	20
3C 396............	1.6	0.07	30	20
G346.6−0.2......	1.5	0.06	29	20
3C 391............	1.4	0.06	28	20
SN 386[a]	1.2	0.05	26	20
RCW 103[a]	1.2	0.05	26	20

NOTE.—Values shown in this table are upper limits, because in each case the bulk of the continuum is assumed to be synchrotron. Values shown in cgs units were rounded to two digits, while their common-unit equivalents were rounded to the more reasonable one significant figure. Note that while 10 μG was assumed for a standard SNR magnetic field, Cas A's magnetic field is about 1 mG (i.e., $E_{max} \sim 8$ TeV), and others are quite uncertain.

[a] Contains a known hard X-ray central source.

[b] This value of $\nu_{rolloff}$ is not a limit but results from the model of the nonthermal X-ray emission by Reynolds (1996). See § 4.

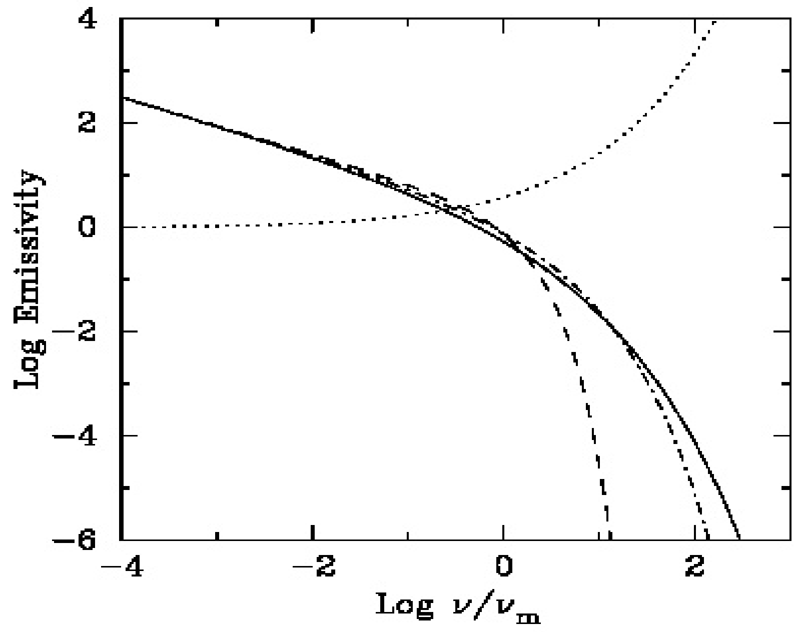

FIG. 1.—Synchrotron emissivity produced by the electron spectrum of eq. (1), with power-law index $s = 2$. The solid line shows the numerical integration of the single-particle emissivity; the dashed line shows the emissivity of an abruptly truncated electron distribution [$N(E) = 0$ for $E > E_{max}$], and the dot-dashed line shows the distribution of eq. (1) convolved with the δ-function approximation to the single-particle synchrotron emissivity. The dotted line shows the log of inverse of the decrement function, the factor by which the cutoff emissivity lies below the power-law extrapolation.

Reynolds & Keohane : 1999, ApJ.525,p368   Young, SNR in Galaxy

● $Do=10^{29}(E/TeV)^{\delta}$ cm^2/s

E=3TeV, Emax =10TeV, 20TeV

$1/bE = T = 0.811 \times 10^5$ yr

Rkpc

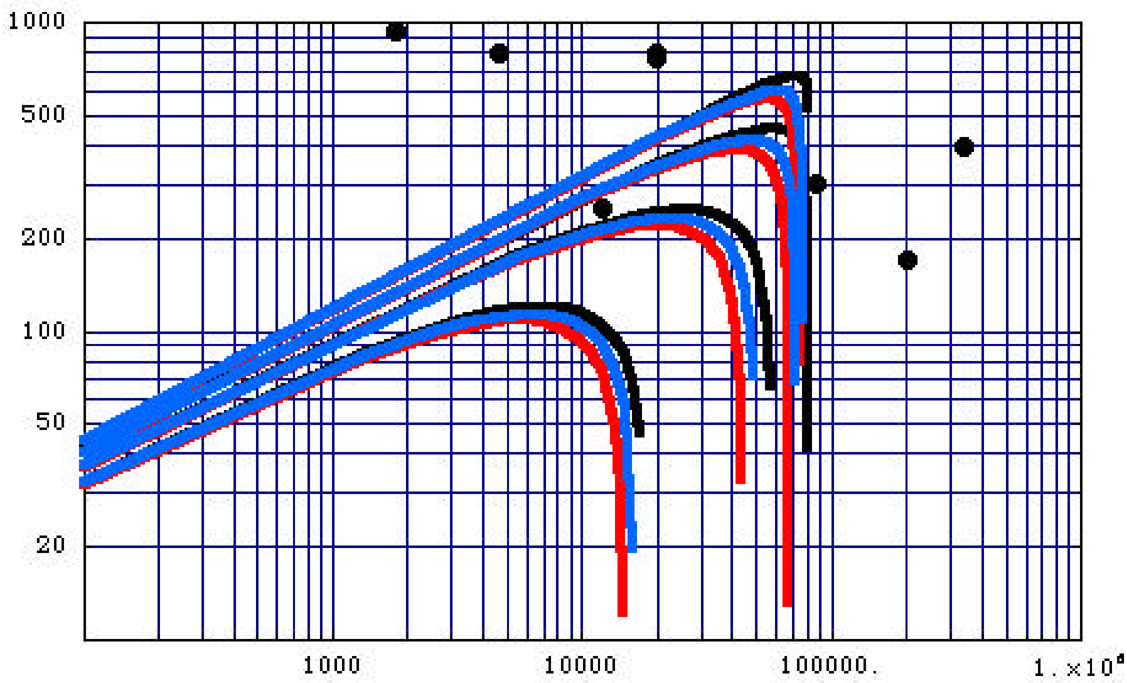

● E=3TeV, Contour Lines are 1.0,10,10^2,10^3 from the top

E2=10TeV

E2=20TeV

E2=∞:No cut

Cosmic-ray Electron Spectra with D values

$D_0 = 1\times10^{29}(\mathrm{cm^2s^{-1}})$

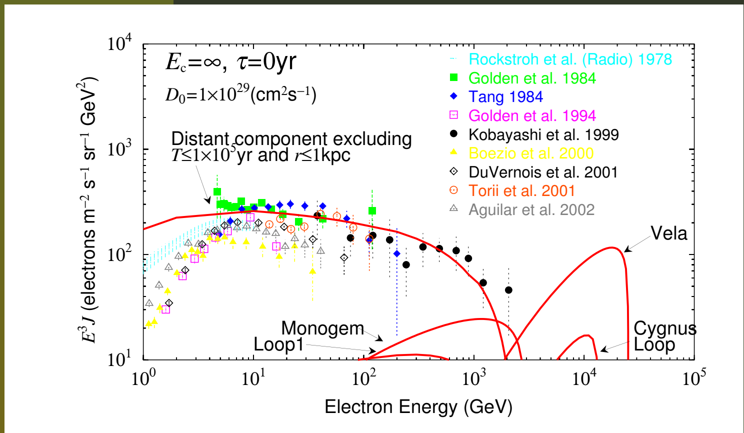

$D_0 = 2\times10^{29}(\mathrm{cm^2s^{-1}})$

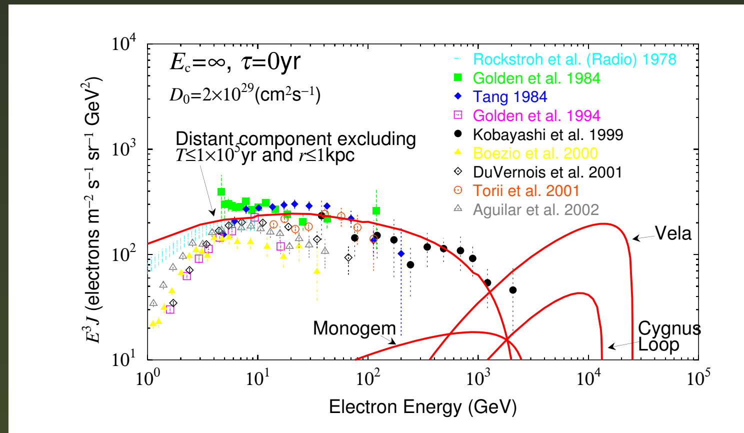

$D_0 = 4\times10^{29}(\mathrm{cm^2s^{-1}})$

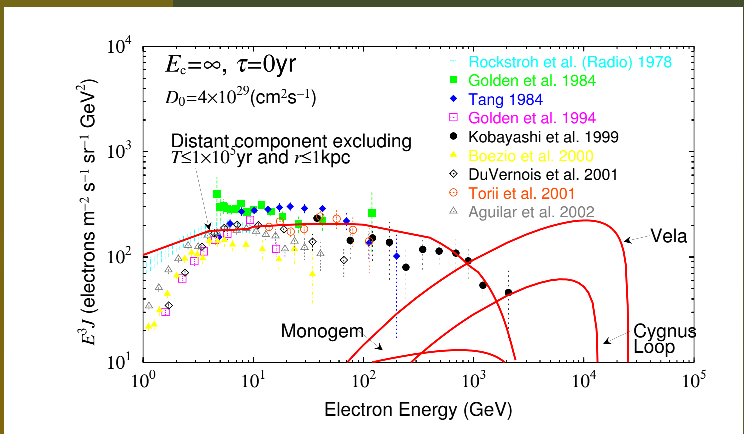

* A power-law source spectrum without cut-off
* Prompt release after the explosion

- The absolute flux and spectral shape change with D.
- The maximum energy of each SNR is same, independent of D.

Electron Spectra with Cut-off Energies

$E_c = \infty$

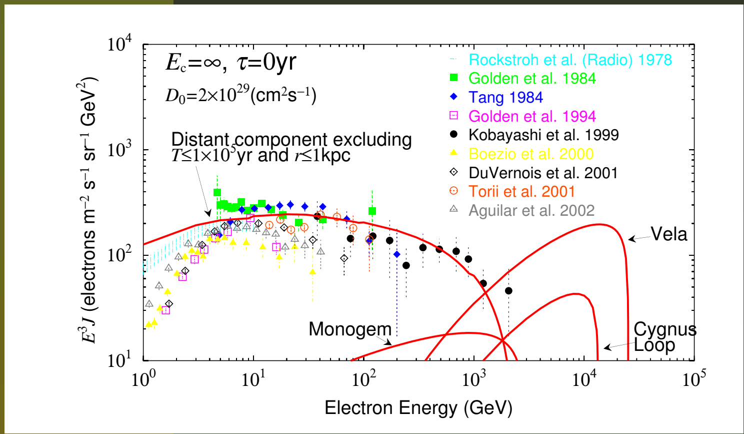

$E_c = 20\mathrm{TeV}$

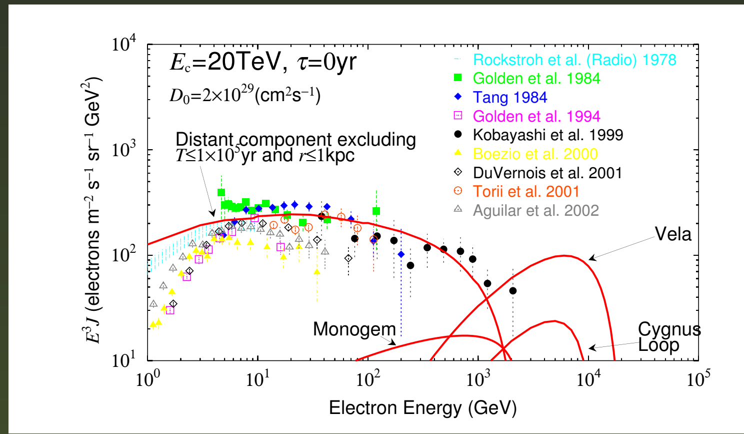

$E_c = 10\mathrm{TeV}$

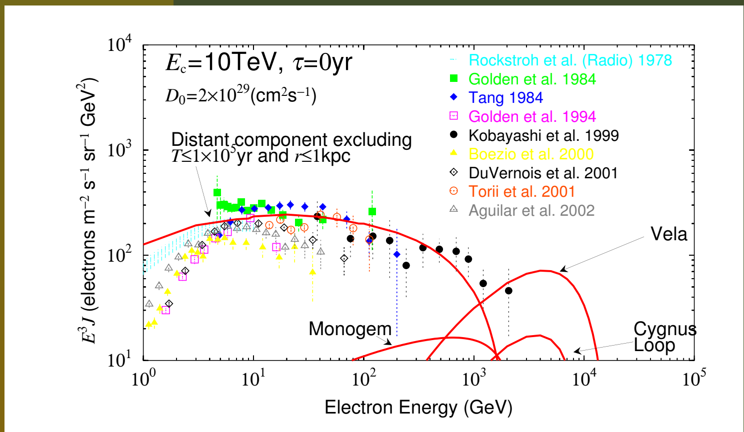

* Prompt release after the explosion

* $D_0 = 2\times10^{29}(\mathrm{cm}^2\mathrm{s}^{-1})$

- The spectra are similar with each other, independent of the cut-off energies.

Electron Spectra with Burst-like Release Times

$\tau = 5\times10^3$yr

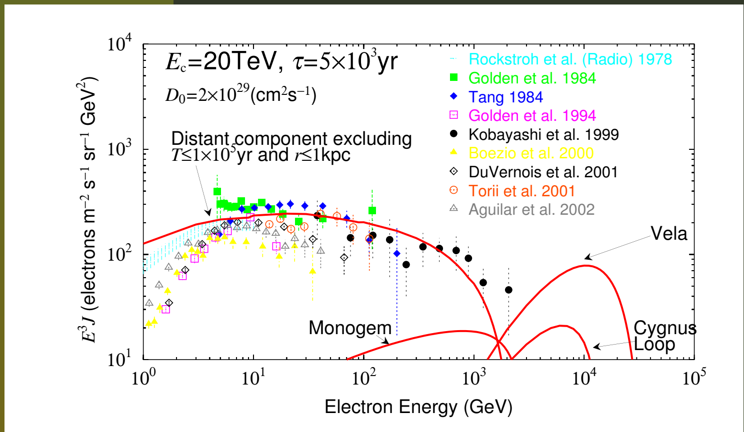

$\tau = 1\times10^4$yr

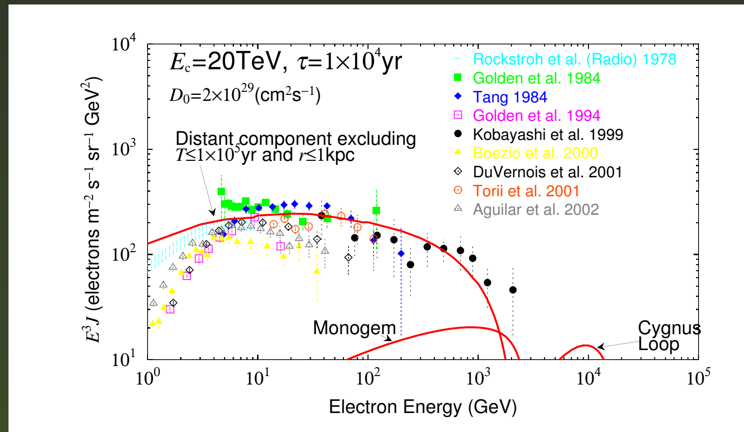

$\tau = 5\times10^4$yr

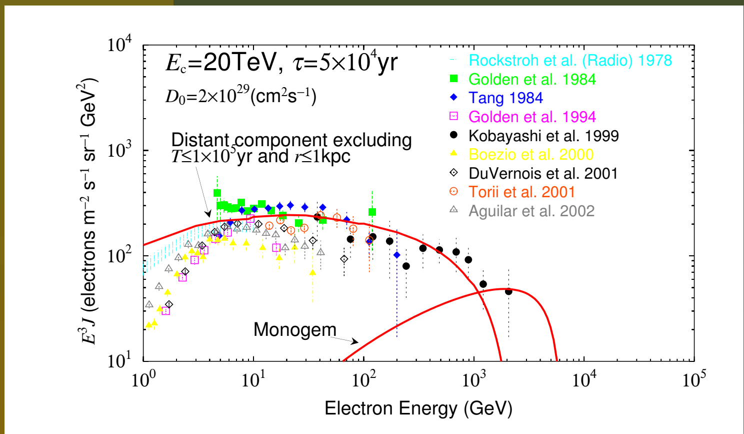

$\tau = 1\times10^5$yr

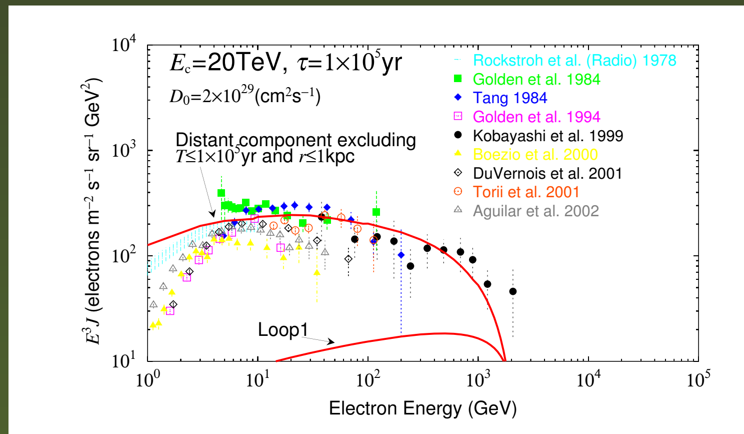

- The delay of the release time from SNRs have a large impact on the flux in the TeV region for $\tau > 1\times10^4$yr.

Electron Spectra with Continuous Release Times

$\tau = 0 - 1{\times}10^4\mathrm{yr}$

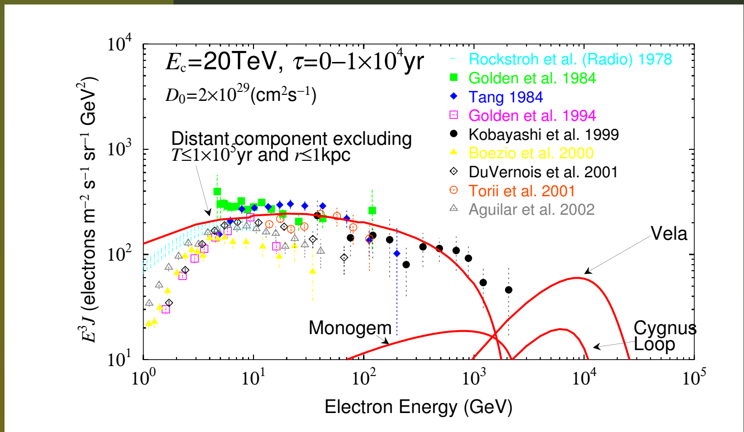

$\tau = 0 - 1{\times}10^5\mathrm{yr}$

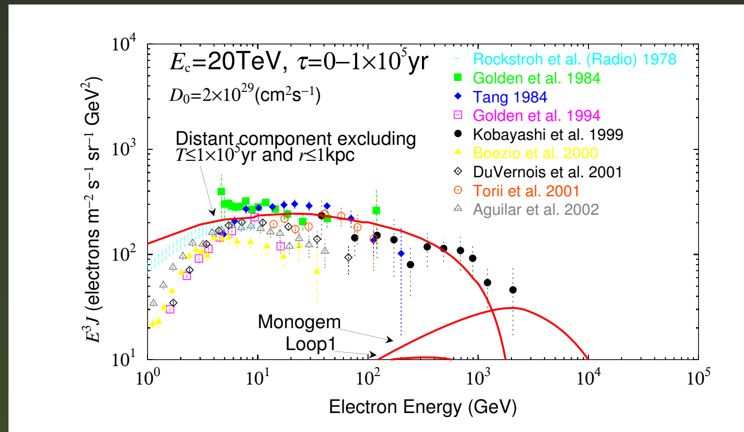

* $E_c = 20\mathrm{TeV}$
* $D_0 = 2{\times}10^{29}(\mathrm{cm^2 s^{-1}})$

- The spectra are well represented by that of the burst-like release with a mean value of the continuous release time.

Summary

- Effect of Delay release

☆No significant Difference in case between τ =0 and 5×10^3yr

Prompt release approximation is good when τ < 5×10^3yr

☆Continuous release from SNR is well approximated by taking appropriate values of τ .

3. Depression of the source spectrum beyond Ec

☆Large depression of flux beyond 10TeV if Ec >20TeV, but

☆No significant depression around a few TeV

★ Main Contributors

Delay of Release	Main Contributors
$\tau = 0\sim 5\times10^3$yr:	Vela, Cygnus Loop
$\tau = \sim 10^4$yr:	Cygnus Loop
$\tau = (2\text{-}5)\ 10^4$yr:	Monogem
$\tau = \sim 10^5$yr:	No clear candidates

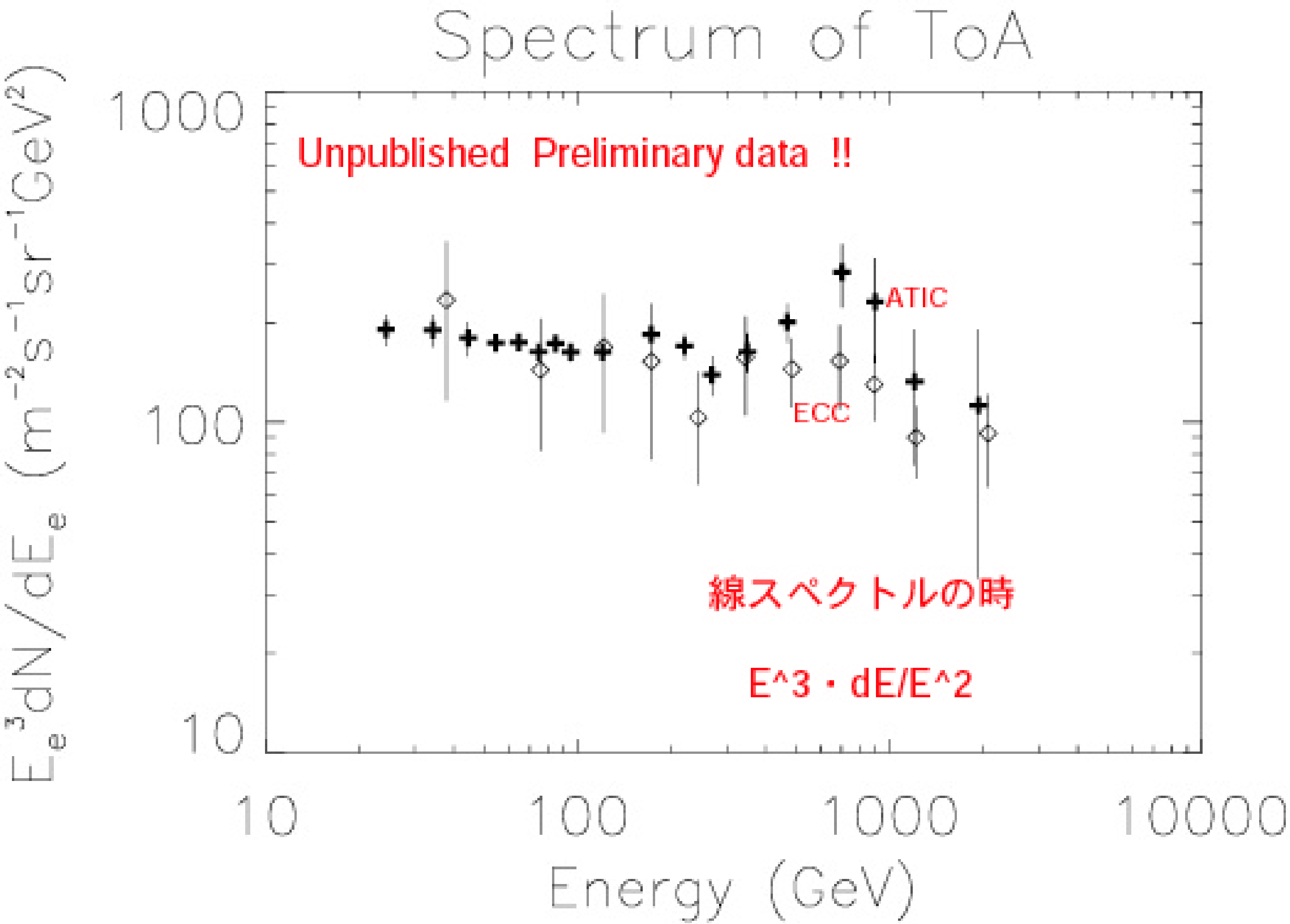
Spectrum of ToA
Unpublished Preliminary data !!
ATIC
ECC
線スペクトルの時
E^3・dE/E^2
1000
100
10
10
100
1000
10000
Energy (GeV)
$E_e^3 dN/dE_e$ ($m^{-2}s^{-1}sr^{-1}GeV^2$)

ECC: Electron Spectrum. 04.1.17. T.K.

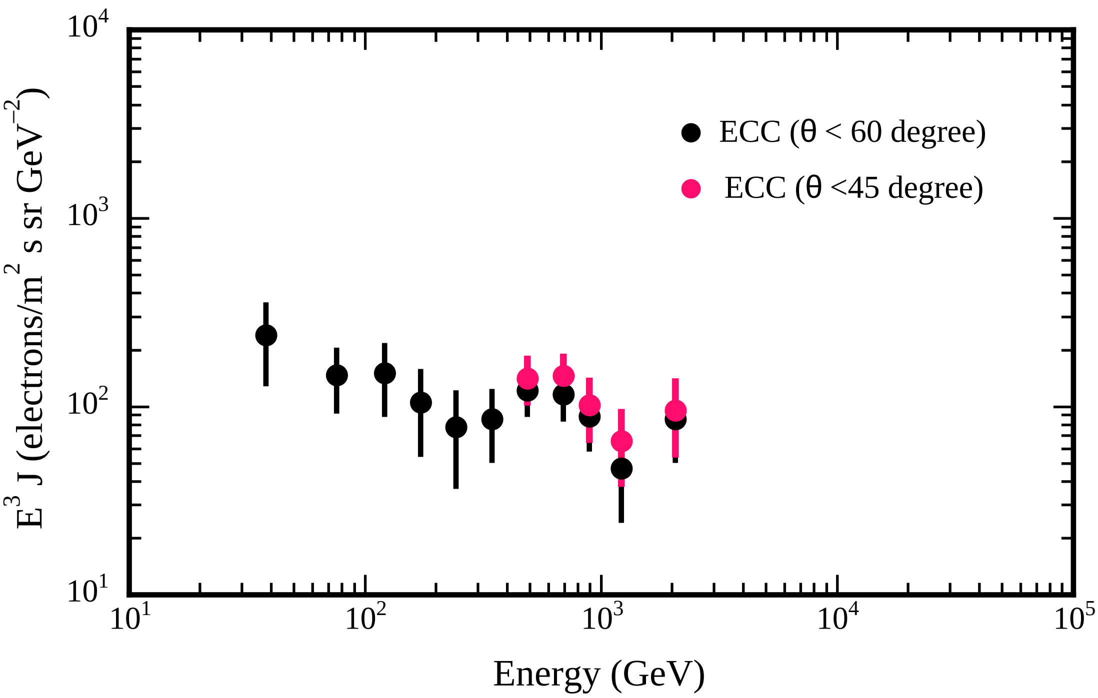

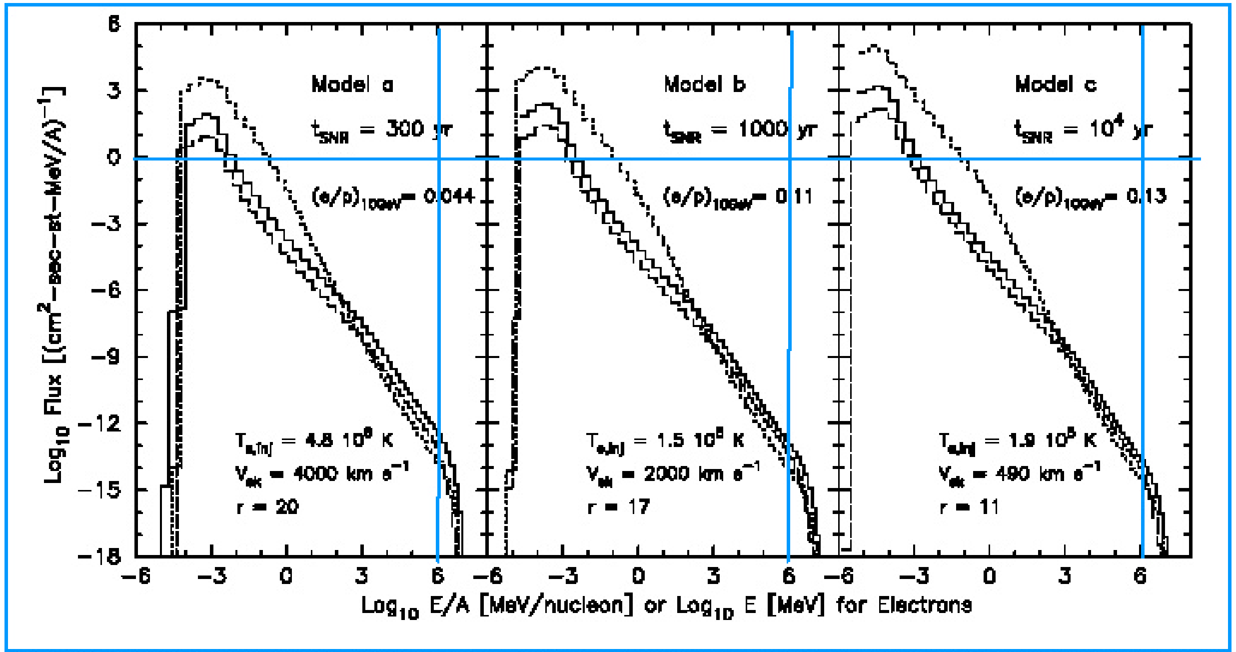

FIG. 5.—Particle omnidirectional fluxes, dJ/dE [particles cm^{-2} s^{-1} sr^{-1} (MeV/A)$^{-1}$], vs. energy per nucleon for ions and vs. energy for electrons ($A \equiv 1$ for electrons), obtained from our example of an expanding remnant in the Sedov phase (see Table 1 for model parameters). All spectra are calculated downstream from the shock in the shock rest frame and are obtained as explained in the text with a steady state approximation. In each panel, the solid and dashed lines show the hydrogen and He^{+2} spectra, respectively, and the dotted line shows the electron spectrum. Both ionic species contribute to the shock smoothing, and the far upstream number density of helium is 1/10 that of hydrogen. The curves are normalized such that $V_{sk} n_{p,1} = 1$ cm^{-2} s^{-1}. The electron spectra are obtained with $E_{crit} = 100$ keV and $f_e = 1$. As the remnant evolves, the shock slows and weakens and the injected electron temperature $T_{e,inj}$ diminishes in accordance with the decline in the dissipative heating of ions (for fixed f_e) in the shock layer.

Barinmg. 1999: ApJ 513,p311

T=10^{4}yr, **Do=10^{29}cm^2/s** **Do=2x10^{29}cm^2/s** **Do=4x10^{29}cm^2/s**

R=100pc

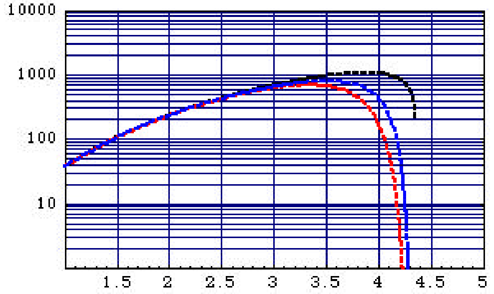

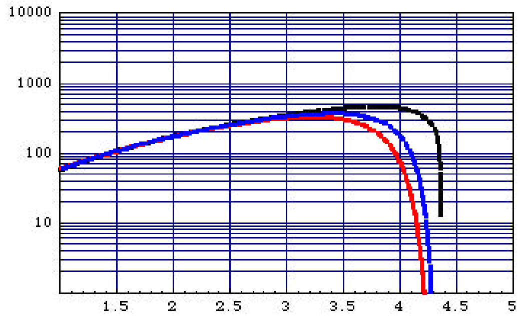

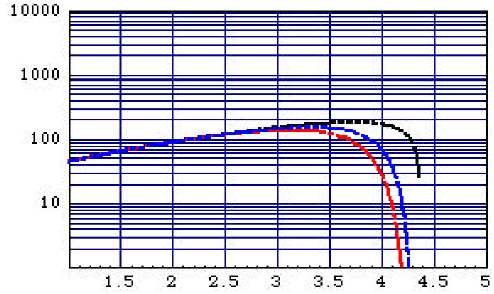

R=200pc

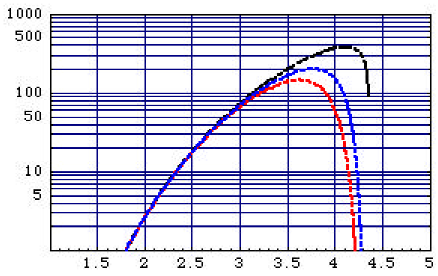

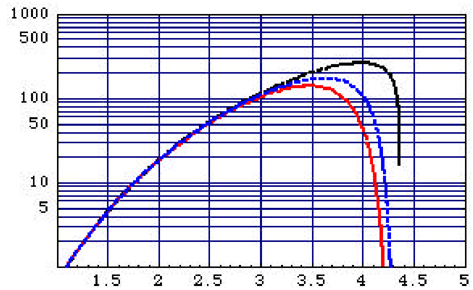

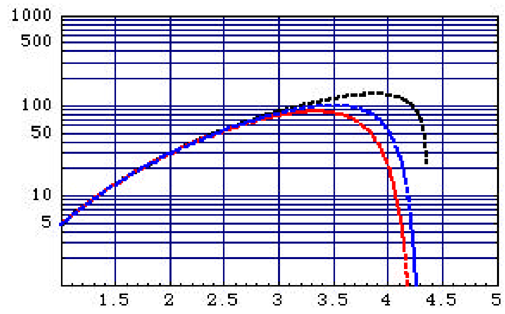

R=300pc

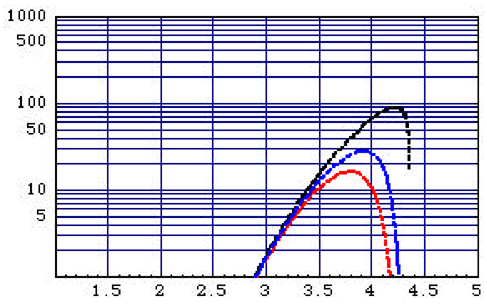

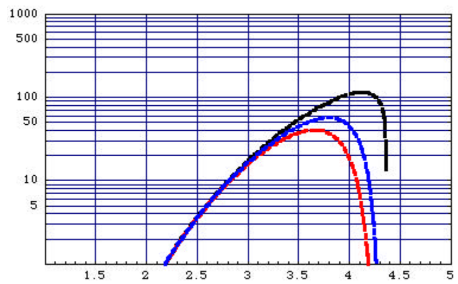

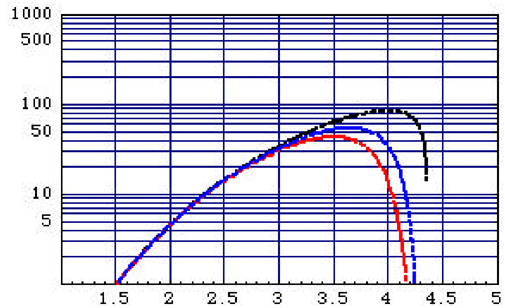

R=400pcR

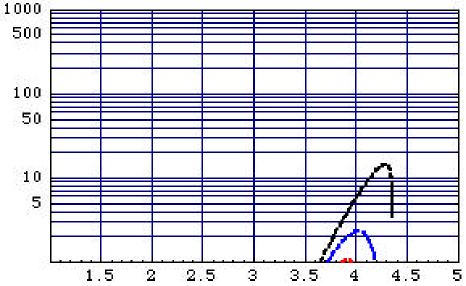

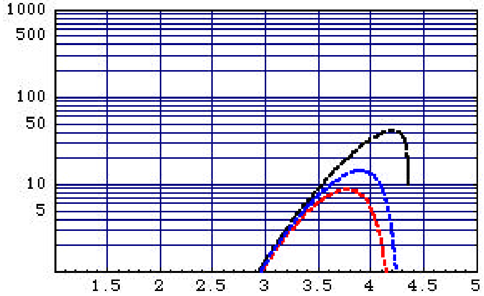

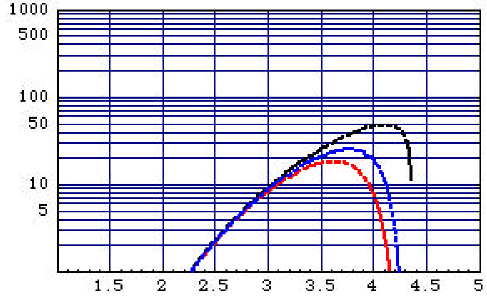

R=500pc

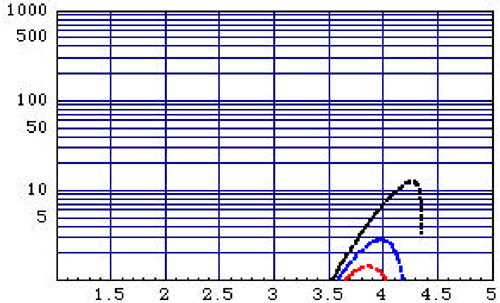

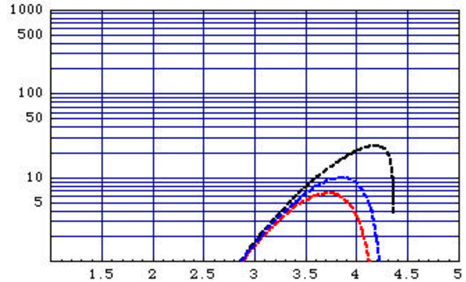

R=600pc

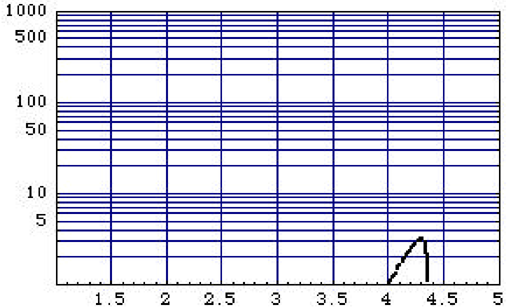

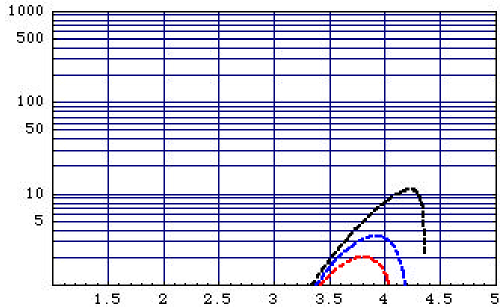

R=700pc

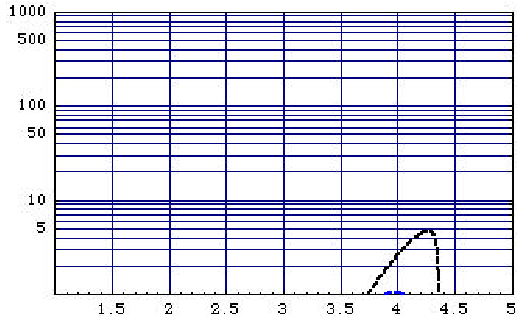

R=800pc